

Analysis of a Linear Design for a Sports Utility Vehicle in Slalom Manoeuvres

Mohd Firdaus Omar¹, Intan Mastura Saadon², Rozaimi Ghazali¹, Mohd Khairi Aripin¹ and Chong Chee Soon¹

¹Centre for Robotics and Industrial Automation, Faculty of Electrical Engineering, Universiti Teknikal Malaysia Melaka, Hang Tuah Jaya, 76100, Durian Tunggal, Melaka, Malaysia

Email: m011610004@student.utm.edu.my, {rozaimi.ghazali, khairiaripin}@utm.edu.my, halklezt@gmail.com

²Faculty of Engineering Technology, Universiti Teknikal Malaysia Melaka, Hang Tuah Jaya, 76100, Durian Tunggal, Melaka, Malaysia

Email: mastura@utm.edu.my

Abstract—In the past two decades, automotive manufacturing has witnessed some advancements, especially for vehicle handling and active safety systems (ASSs). Progressively, more controllers have been designed to deal with linear and non-linear systems. However, studies and research on integral terms in linear quadratic regulators are scarce. In this paper, linear controllers, including the proportional integral derivative (PID) and linear quadratic integral (LQI) using direct yaw control (DYC), have been designed and compared. With the interference of external disturbances and variation of the friction coefficient, the result indicates that the LQI controller produces a significant improvement in the vehicle slalom manoeuvre system compared to the PID controller.

Index Terms—direct yaw moment, disturbance, linear quadratic integral, slalom manoeuvre

I. INTRODUCTION

In the past two decades, there have been advancements in technology in the automotive sector, especially in vehicle handling and safety systems. For example, a system called Advanced Driver Assistance has been studied in [1], where the system warns the driver or a steering intervention system takes control when the vehicle is in a dangerous situation, using sensors or image processing technology. In [2, 3], the Global Positioning System was used to control the vehicle or estimate the sideslip angle of the vehicle, whether for a semi- or a fully autonomous vehicle. Active Safety Systems (ASSs) are another type of system that has been widely studied, where the vehicle is regulated using the available sensors and is directly controlled during critical situations using actuators [4].

ASSs, mostly called electronic stability control, have several types of control to improve the handling of vehicles, such as differential braking control (DBC), sometimes called direct yaw control (DYC); steering intervention (active steering/steer by wire); active anti-roll bar and independent all-wheel-drive torque vectoring distribution. In this research, the DYC method is implemented because this system has been improved since the inception of the anti-lock braking system (ABS) and most car manufacturers have been widely using this

method because of its cost-effectiveness, as reported in [5].

In order to improve this method, many researchers have proposed different control strategies for improving vehicle systems during hard cornering or critical situations. In general, control design can be divided into two categories: linear and non-linear. For example, in [6], a non-linear SMC method was proposed to achieve fault-tolerant control in order to avoid the strong coupling effect between individual control targets in an electric vehicle. In [7], the authors proposed a second-order sliding mode observer, finite-time control technique (non-smooth controller) and non-linear disturbance observer in order to suppress the lumped disturbance, uncertainties and external disturbances. Another non-linear control design is artificial intelligence. In [8], fuzzy logic control (FLC) was presented to coordinate the engine torque and active brake pressure for uneven low-friction road conditions. The authors of [9] proposed an integrated ABS with an electronic stability programme based on the FLC method in order to verify the robustness against a variety of road profiles and surfaces. In advanced non-linear control design, the control structure is added with another controller, hence called a hybrid controller. For instance, the work done in [10], where at upper level controller has PID control, FLC PID control and FLC control to calculate the desired value of yaw rate, traction force and torque input of four-wheel motor. In another study [11], an FLC with an SMC was proposed, where the SMC is used to design a discrete-time model and the FLC is used to solve the boundary layer width. As a result, the control design was improved to the network-induced delay, which is robust against model uncertainties, system parameter variations and external disturbances.

In this paper, we focus on the linear control design because, in the real world, most manufacturers are still using a linear design because of its simplicity, transparency, reliability and cost-effectiveness, as reported in [12]. Some non-linear control designs are complicated to implement, but they can yield the best results to overcome model uncertainties, parameter variations, external disturbances or control effort, as

discussed above. Therefore, the linear design remains to be deeply studied in order to improve the robustness of vehicle systems. In the linear control design, the most widely used controller in industry is the proportional integral derivative (PID) controller because of its ability to achieve a large reduction in CPU utilisation with a minor degradation of control performance, as mentioned in [13]. Many researchers have proposed different control designs. For example, in [14], an independent four-wheel-drive vehicle using the DYC method was implemented for torque distribution in order to prevent wheel slip and loss of stability. The authors of [15] utilised optimal control allocation for distributing the active yaw moment in order to lower the workload of the actuator. Another example is given in [16], where a pre-control method was utilised by hierarchical pre-control logic and integrated with DYC in order to improve the control effect and reduce the control effort.

Another widely used linear design is the linear quadratic regulator (LQR), which is based on the optimal control theory. The advantages of this control technique are that it can guarantee the stability of a certain bandwidth and it possesses a number of desirable constraints and satisfies a number of properties demanded by the designer of the control system, as mentioned in [17]. In [18], a hierarchical control strategy was proposed by integrating a feedforward and feedback control part to reduce the object of the stability yaw moment in the upper controller. In [19], integrated vehicle longitudinal and lateral stability was utilised to improve the steerability and minimise the control effort, based on the optimal control theory. In [20], an LQR controller was utilised by the integrated control of DYC and front steering angle for the efficacy of a vehicle system using Modelica software. However, linear designs mostly have a drawback related to the robustness of overcoming model uncertainties, parameter variations or external disturbances. According to [21], by introducing an integral term in the system parameters of the LQR, the offset of the control system can be eliminated, making it more robust in overcoming external disturbances, unmodelled dynamics or measurement noises. However, less study involves in LQI controller with interference of external disturbance during critical manoeuvre in this system. Thus, in this paper, a comparison of the linear design between an LQI and a PID controller is proposed in order to investigate the effectiveness toward SUV parameters and external disturbances.

This paper is organised as follows. In Section II, a vehicle dynamic model is presented. In Section III, the controller design and structure are explained. The computer simulation results using MATLAB/Simulink are presented along with a discussion in Section IV. At the end, our final remarks are given in Section V.

II. VEHICLE DYNAMIC MODEL

The vehicle model shown in Fig. 1 is used to study and simulate the behaviour of a vehicle's motion during various manoeuvres. In this study, a three-degree-of-freedom (3-DOF) non-linear model is used to represent

the dynamics of SUV handling. The non-linear vehicle dynamics consist of the sideslip angle and the longitudinal, lateral and yaw motion.

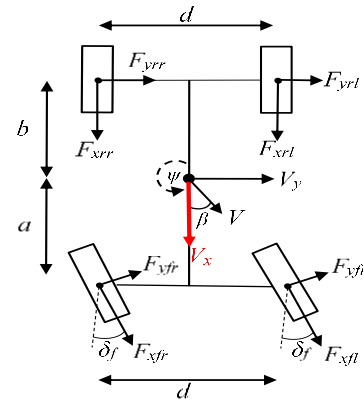


Figure 1. Non-linear vehicle model.

The parameter of SUV is variant because of the changes of tyre-road friction coefficient (μ) and manoeuvring. In this paper, the tyre-road friction coefficient and steering angle are considered to be independent uncertainty parameters. The equations of longitudinal, lateral and yaw motions of a vehicle body can be described as follows:

$$\begin{aligned} ma_x &= m(\dot{v}_x - rv_y) \\ &= (F_{xfl} + F_{xfr})\cos(\delta_f) + F_{xrl} \dots, \quad (1) \\ &\dots + F_{xrr} - (F_{yfl} + F_{yfr})\sin(\delta_f) \end{aligned}$$

$$\begin{aligned} ma_y &= m(\dot{v}_y + rv_x) \\ &= (F_{yfl} + F_{yfr})\cos(\delta_f) + F_{yrl} + \dots, \quad (2) \\ &\dots + F_{yrr} + (F_{xfl} + F_{xfr})\sin(\delta_f) \end{aligned}$$

$$\begin{aligned} I_z \dot{r} &= a(F_{xfl} + F_{xfr})\sin(\delta_f) + \dots \\ &\dots + a(F_{yfl} + F_{yfr})\cos(\delta_f) - \dots, \quad (3) \\ &\dots + b(F_{yfl} + F_{yrr}) + M_z \end{aligned}$$

where the longitudinal tyres' forces are denoted as F_{xfl} for the front left tyres, F_{xfr} for the front right tyres, F_{xrl} for the rear left tyres and F_{xrr} for the rear right tyres. The lateral forces of the front left, front right, rear left and rear right tyres are given by F_{yfl} , F_{yfr} , F_{yrl} and F_{yrr} , respectively. The front wheel steer angle and vehicle velocity are represented as input denoted by δ_f and v_x . The yaw rate (r) and sideslip angle (β) are output variables that need to be controlled. The distances from the front and the rear to the centre of gravity (CG) are referred as the a and b parameters. The vehicle's width track, yaw moment and lateral velocity are denoted as d , M_z and v_y , respectively. Other parameters that must be taken into account are vehicle mass (m), moment of inertia (a) and cornering stiffness (I_z) at the front and rear (C_f and C_r).

Using the two-track model as a reference, the variable yaw rate (r) from Eq. (3) can be expressed as follows:

$$\dot{r} = \frac{1}{I_z} \left[a \begin{pmatrix} F_{yfl} \cos \delta_f + F_{yfr} \cos \delta_f + \dots \\ \dots + F_{xfl} \sin \delta_f + F_{xfr} \sin \delta_f \\ \dots (-b(F_{yrl} + F_{yrr}) + M_z) \end{pmatrix} + \dots \right] \quad (4)$$

whereas the variable of sideslip (β) can be obtained as follows:

$$\dot{\beta} = \frac{1}{m_v} \begin{bmatrix} \cos \beta (\cos \delta_f (F_{xfl} + F_{xfr}) + \dots) \\ -\sin \delta_f (F_{yfl} + F_{yfr}) - \dots \\ \sin \beta (\sin \delta_f (F_{xfl} + F_{xfr}) + \dots) \\ -\sin \delta_f (F_{yfl} + F_{yfr}) \end{bmatrix} - r \quad (5)$$

The tires tend to turn at the z -axis when the yaw moment is bigger than zero. The yaw rate (r) and sideslip (β) can be determined by lateral acceleration (a_y) in forward speed (v) as follows:

$$a_y = \dot{v}_y + rv_x = v(r + \dot{\beta}) \quad (6)$$

The slip angle or sideslip angle is the angle between the actual travel of the wheel's rolling direction and the direction where the wheel is pointing. In order to define the sideslip angle at the front and rear tyres, the following equations are used:

$$a_f = \delta - \frac{\dot{y} + a\dot{\psi}}{\dot{x}} \quad (7)$$

$$a_r = -\frac{\dot{y} - b\dot{\psi}}{\dot{x}} \quad (8)$$

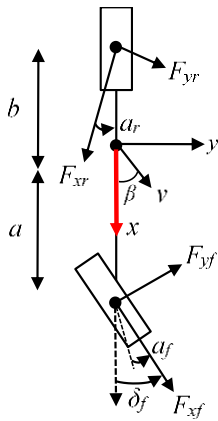


Figure 2. Bicycle model.

The 2-DOF or bicycle model shown in Fig. 2 is used to build the equation of the desired model because it has the simplest form of planar motion and it can be only used to analyse the lateral and yaw motions. In the bicycle model form, there are certain assumptions and parameters that need to be neglected, such as the fixed/constant forward speed, tyre forces operating in the linear region, two front wheels having the same steering angle, the CG not being shifted during the change of the vehicle mass, small angle

approximation, self-alignment torque wheel being negligible, two wheels at the front and rear being combined to become one single unit and the width track being ignored. The configuration of the SUV consists of a front wheel drive with negligible wheel dynamics. Therefore, the lateral and yaw motions for the bicycle model can be described as follows:

$$mv(\dot{\beta} + r) = (F_{yf} + F_{yr}) - r \quad (9)$$

$$I_z \dot{r} = a(F_{yf} - b)F_{yr} \quad (10)$$

The bicycle model is indicated as having a linear characteristic. Therefore, using Eqs. (6) and (7), the cornering stiffness for the front and rear tyres can be obtained by the following equations:

$$F_{yf} = C_f a_f \quad (11)$$

$$F_{yr} = C_r a_r \quad (12)$$

Using the linear state space model, the differential equation of variable yaw rate and sideslip can be obtained by rearranging and simplifying Eqs. (7)–(12) as follows:

$$\dot{x} = Ax + Bu,$$

$$\begin{bmatrix} \dot{\beta} \\ \dot{r} \end{bmatrix} = \begin{bmatrix} a_{11} & a_{12} \\ a_{21} & a_{22} \end{bmatrix} \begin{bmatrix} \beta \\ r \end{bmatrix} + \begin{bmatrix} b_{11} & b_{12} \\ b_{21} & b_{22} \end{bmatrix} u, \quad (13)$$

where

$$\begin{aligned} a_{11} &= \frac{C_f a - C_r b}{mv_x^2}, & a_{12} &= \frac{C_f + C_r}{mv_x}, \\ a_{21} &= \frac{C_f a^2 - C_r b^2}{I_z v}, & a_{22} &= \frac{C_r b - C_f a}{I_z}, \\ b_{11} &= \frac{C_f}{mv}, & b_{12} &= 0, \\ b_{21} &= \frac{C_f a}{I_z}, & b_{22} &= \frac{1}{I_{zz}}. \end{aligned}$$

The sideslip angle $\beta(s)$ and yaw rate $r(s)$ can be expressed by implementing the Laplace transform into the state space equation as follows [25]:

$$B(s) = \frac{\begin{pmatrix} (b_{11}s - a_{22}b_{11} + a_{12}b_{11} + \dots) \\ + a_{12}b_{21} \end{pmatrix} \delta + (a_{12}b_{22})M}{(s - a_{11})(s - a_{22}) - a_{12}a_{21}}, \quad (14)$$

$$r(s) = \frac{\begin{pmatrix} (a_{21}b_{11} + b_{21}s + a_{11}b_{21})\delta_f(s) + \dots \\ \dots - (a_{11}b_{22} - b_{22}s)M(s) \end{pmatrix}}{(s - a_{11})(s - a_{22}) - a_{12}a_{21}} \quad (15)$$

The design of feedforward compensation in the vehicle model minimises or makes the vehicle's sideslip angle become zero. Therefore, the relationship between the two control inputs, direct yaw moment $M(s)$ and front steering angle $\delta_f(s)$, is assumed as follows:

$$M(s) = P_{ff} \cdot \delta_f(s), \quad (16)$$

where P_{ff} is the proportional feedforward gain.

By solving Eqs. (14) and (15), the result of the feedforward gain can be obtained as follows:

$$P_{ff} = \frac{b_{11} \cdot a_{22} - b_{21} \cdot a_{12}}{a_{12} \cdot b_{22}}. \quad (17)$$

The transfer function of the yaw rate with respect to the front steering angle can be obtained by substituting Eqs. (17) and (16) into Eq. (15) as follows:

$$\gamma(s) = \frac{\left(\begin{array}{l} b_{11} \cdot a_{22} \cdot s + \dots \\ \dots + (b_{11} \cdot a_{12} \cdot a_{21} - b_{11} \cdot a_{11} \cdot a_{22}) \end{array} \right)}{a_{12} \left[\begin{array}{l} s^2 - (a_{11} + a_{12})s + \dots \\ \dots + a_{11} \cdot a_{12} - a_{12} \cdot a_{21} \end{array} \right]} \delta_f(s). \quad (18)$$

The desired vehicle model or bicycle model (2-DOF) is used as a reference of the yaw rate and can be modelled on the first-order delay system. By setting $\dot{\beta}$ and $\dot{\gamma}$ equal to zero and solving γ in Eq. (13), the expression is obtained as follows:

$$X_d = \begin{bmatrix} \beta_d \\ \gamma_d \end{bmatrix} = \begin{bmatrix} 0 \\ \frac{\gamma_{ssg}}{\tau_r s + 1} \end{bmatrix} \delta_f, \quad (19)$$

where γ_{ssg} is the steady-state yaw rate gain and τ_r is the delay time constant.

As for the sideslip angle, the desired model is designed to have a zero value at steady state because the tyre becomes skidded when the angle of sideslip gets bigger.

By comparing Eqs. (19) and (18), the steady state of the yaw rate gain can be obtained as follows:

$$\gamma_{ssg} = \frac{b_{11}(a_{12} \cdot a_{21} - a_{11} \cdot a_{22})}{a_{12}(a_{11} \cdot a_{22} - a_{12} \cdot a_{21})}. \quad (20)$$

Then, the desired vehicle model can be expressed as in the following expression:

$$\dot{X}_d = A_d \cdot X_d + E_d \cdot \delta_f. \quad (21)$$

III. CONTROLLER DESIGN

The tyre–road coefficient, external disturbance and steering angle can affect the handling and stability of the vehicle during critical manoeuvres. Thus, this will make the yaw rate and sideslip angle of the vehicle become unstable. As discussed in Section I, the DYC technique is used in this research for the control of the yaw rate and sideslip angle in order to stabilise and maintain the vehicle in a proper response during critical dynamic behaviours. The objective of the control system is to make the actual vehicle model follow the desired vehicle model by calculating the value of the yaw rate (γ) and follow the desired value of the yaw rate (γ_d). The purpose

of controlling the sideslip angle is to prevent the vehicle from slipping or the wheel is uncontrolled from the pointed direction of the wheel by limit the sideslip angle (β). By regulating the slip ratio of the wheel between the differences of the left and right tyre longitudinal forces, the yaw moment can be generated to stabilise the vehicle using the DYC control technique.

The state equation [Eq. (13)] needs to be transformed in order to design the feedback controller as shown in the expression below:

$$\begin{bmatrix} \dot{\beta} \\ \dot{\gamma} \end{bmatrix} = \begin{bmatrix} a_{11} & a_{12} \\ a_{21} & a_{22} \end{bmatrix} \begin{bmatrix} \beta \\ \gamma \end{bmatrix} + \begin{bmatrix} e_1 \\ e_2 \end{bmatrix} \delta_f + \begin{bmatrix} b_1 \\ b_2 \end{bmatrix} M, \quad (22)$$

where

$$e_1 = -\frac{C_f}{mv_x}, \quad e_2 = \frac{C_f l_f}{I_{zz}},$$

$$b_1 = 0, \quad b_2 = \frac{1}{I_{zz}}.$$

Therefore, the new state equation is

$$\dot{X} = A \cdot X + B \cdot M + E \cdot \delta_f. \quad (23)$$

By assuming the difference between the ideal model and the actual model as an error (e) and by differentiating this error in Eq. (24), the expression becomes as shown in Eq. (25).

$$e = X - X_d, \quad (24)$$

$$\dot{e} = \dot{X} - \dot{X}_d. \quad (25)$$

Equations (21) and (23) are substituted into Eq. (25), yielding Eq. (26). By simplifying Eq. (26), we obtain Eq. (27).

$$\begin{aligned} \dot{e} = & A \cdot X - A \cdot X_d + A \cdot X_d - \dots \\ & \dots + A_d \cdot X_d + B \cdot M + E \cdot \delta_f - E_d \cdot \delta_f, \end{aligned} \quad (26)$$

$$\dot{e} = A e + B \cdot M + (A - A_d) \cdot X_d + (E - E_d) \cdot \delta_f. \quad (27)$$

The third part, $(A - A_d) \cdot X_d$, and fourth part, $(E - E_d) \cdot \delta_f$, in Eq. (29) can be treated as a disturbance (W) by front wheel steering, and the final equation becomes

$$\dot{e} = A e + B \cdot M + W. \quad (28)$$

A. Design of the Linear Quadratic Integral (LQI)

The optimal control theory is one of the methods for improving any given system of control law. Based on this control theory, the system can achieve optimal criteria as desired. The LQI controller is a variation of the LQR controller, where the control law stems from solving the Riccati function in the LQR framework with added integral regulation of the output variable. In order to design the linear quadratic integrator, first, Eq. (28) is differentiated, yielding the following equation:

$$\ddot{e} = A\dot{e} + B\dot{M} + \dot{W}. \quad (29)$$

Then, the equation is expanded to Eq. (30) and simplified to Eq. (31) as follows:

$$\frac{d}{dt} \begin{bmatrix} \dot{E} \\ E \end{bmatrix} = \begin{bmatrix} A & 0 \\ 1 & 0 \end{bmatrix} \begin{bmatrix} \dot{E} \\ E \end{bmatrix} + \begin{bmatrix} B \\ 0 \end{bmatrix} \dot{M} + Z, \quad (30)$$

$$\dot{X}_r = A_r X_r + B_r \dot{M} + Z, \quad (31)$$

where

$$X_r = \begin{bmatrix} \dot{\beta} - \beta_d \\ \dot{\gamma} - \gamma_d \\ \beta - \beta_d \\ \gamma - \gamma_d \end{bmatrix} A_r \begin{bmatrix} \frac{C_f l_f}{mv_x^2} & \frac{C_f + k_r}{mv_x} & 0 & 0 \\ \frac{C_f l_f^2}{I_{zz} V_x} & \frac{C_f l_f + C_r l_r}{I_{zz}} & 0 & 0 \\ 1 & 1 & 0 & 0 \\ 1 & 1 & 0 & 0 \end{bmatrix},$$

$$B_r = \begin{bmatrix} 0 \\ 1 \\ I_z \\ 0 \end{bmatrix}.$$

The disturbance of Z in Eq. (31) will be equal to zero. Based on the optimal control theory, the new state feedback will be

$$\dot{M} = - \begin{bmatrix} G_{fb1}(\dot{\beta} - \dot{\beta}_d) + G_{fb2}(\dot{\gamma} - \dot{\gamma}_d) + \dots \\ \dots + G_{fb3}(\beta - \beta_d) + G_{fb4}(\gamma - \gamma_d) \end{bmatrix}. \quad (32)$$

where G_{fb} is the feedback gain that is used to minimise the quadratic cost function (J) as in the following equation:

$$J = \int_0^{\infty} (X_r^T Q X_r + \dot{M}^T R \dot{M}) dt. \quad (33)$$

Then, the total yaw moment can be summed up as follows:

$$M_{zT} = M(s) \dot{M}. \quad (34)$$

For fast convergence of the error, the value of Q should be bigger than that of R .

B. Design of the PID

The PID controller is one of the feedback mechanism controllers, which involves three-term or parameter control, that is, proportional (K_p), integral (K_i) and derivative (K_d). Each parameter of the PID needs to be tuned in order to make the system fully optimised, as desired by the designer. For example, by controlling the proportional controller (K_p) gain, the rise time (T_r) and steady-state error (SSE) will decrease, but the percentage of overshoot (O_s) will increase, same as the integral controller (K_i) where the rise time will decrease and the SSE of the system is eliminated, but the backlash will increase the percentage of O_s and affect the settling time

(T_s). In order to overcome the overshoot and stabilise another parameter, the derivative gain (K_d) is introduced. The derivative gain can decrease T_s and O_s of the system, but it has a small effect on T_r and SSE.

(i) *PID controller of the yaw rate:*

$$e_i = \gamma_n - \gamma, \quad (35)$$

$$\Delta M_{\gamma n} = K_p^{\gamma n} .e_y(t) + K_i^{\gamma n} + \dots + \int_0^t e_{\gamma n}(t) dt + K_d^{\gamma n} \frac{d[e_{\gamma n}(t)]}{dt}. \quad (36)$$

(ii) *PID controller of the sideslip angle:*

$$e_i = \beta_n - \beta, \quad (37)$$

$$\Delta M_{\beta n} = K_p^{\beta n} .e_y(t) + K_i^{\beta n} + \dots + \int_0^t e_{\beta n}(t) dt + K_d^{\beta n} \frac{d[e_{\beta n}(t)]}{dt}. \quad (38)$$

The tuning method is important for obtaining the desired result. There are various types of tuning methods that can be used, such as manual tuning, Ziegler–Nichols method, Tyreus–Luyben method and Cohen–Coon method. In this research, the auto-tuning method is applied using a toolbox in MATLAB/Simulink, since this method can reduce the time consumption, is easy to implement and can ensure the best operation control scheme in determining the set of controller’s gains.

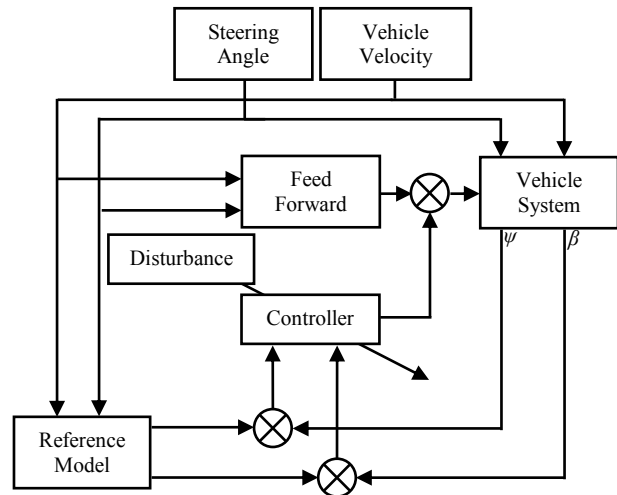


Figure 3. Block diagram of the vehicle system.

IV. ANALYSIS AND RESULT

In order to study and evaluate the performance of the controller, a computer simulation using MATLAB/Simulink was carried out. Fig. 3 shows the overall block model diagram of the vehicle system, and the slalom performance test is carried out to evaluate the controller. Table I lists the parameters of the vehicle taken from [22].

TABLE I. PARAMETERS OF THE SUV.

Symbol	Parameter (unit)	Value
m	Mass (kg)	1,592
C_f	Front cornering stiffness (N/rad)	-68,420
C_r	Rear cornering stiffness (N/rad)	-68,420
H	CG height (m)	0.72
I_{zz}	Yaw inertia ($\text{kg}\cdot\text{m}^2$)	2,488
l_f	Distance from CG to front axle (m)	1.18
l_r	Distance from CG to rear axle (m)	1.77
v	Vehicle speed/velocity (km/h)	100

The slalom test performance is often used to evaluate the vehicle's stability, which can reflect the ability and handling of the vehicle system during large angle cornering motions [23]. Manoeuvres are conducted under two different conditions: a dry road with a road friction coefficient of 1.0μ and a wet road with a road friction coefficient of 0.5μ . In order to make the controller reach the maximum capability and better performance analysis on each controller, the vehicle system is injected with a crosswind disturbance starting at 4 s and ending at 7 s, as shown in [24], and the test is started with a normal speed of 100 km/h. The root mean square error (RMSE) method is employed to compare and verify the performance analysis on each controller because of the difficulty of observing the slalom test manoeuvre.

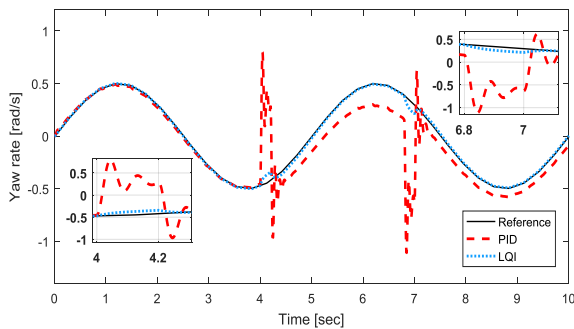


Figure 4. Yaw rate performance on a dry road.

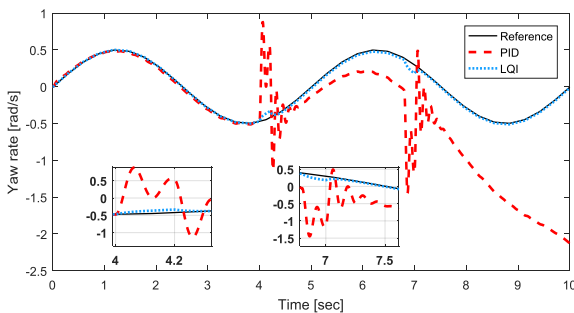


Figure 5. Yaw rate performance on a wet road.

In Fig. 4, the result for the yaw rate on a dry road shows that both controllers are capable of tracking the reference for slalom manoeuvres until it reaches 4 s, where the external disturbance is injected into the system, ending at 7 s. During this period, the PID controller cannot track the reference, and a larger error is obtained until the end of the test. As compared to the LQI controller, the tracking performance is obviously better and the external disturbance is overcome until the end of the test. Fig. 5 shows the result of the yaw rate on a wet

road, where, obviously, the PID controller cannot overcome the external disturbance and has a larger error that can cause the vehicle to lose stability. The LQI controller still can overcome the external disturbance much better than the PID controller does, and it has a better tracking performance until the end of the test.

TABLE II. COMPARISON PERFORMANCE RMSE FOR YAW RATE.

Yaw rate	PID	LQI
Dry road (1.0μ)	2.428224	0.155500
Wet road (0.5μ)	12.02630	0.258184

Table II shows a comparison of the RMSE between the PID and the LQI controllers, where, under dry road conditions, the LQI has a lower RMSE compared to the PID controller. Under wet road conditions, obviously, the PID controller loses controllability because of the larger RMSE, making the vehicle unstable. The RMSE of the LQI controller increases by about 60%, but it can still be considered as controllable because the vehicle does not lose controllability until the end of the test.

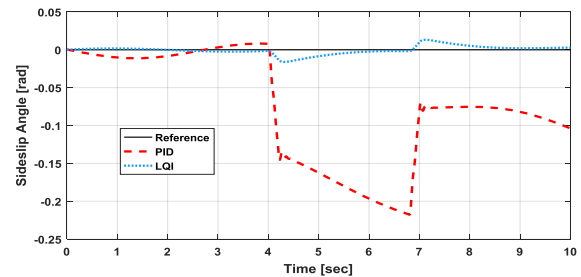


Figure 6. Sideslip angle performance on a dry road.

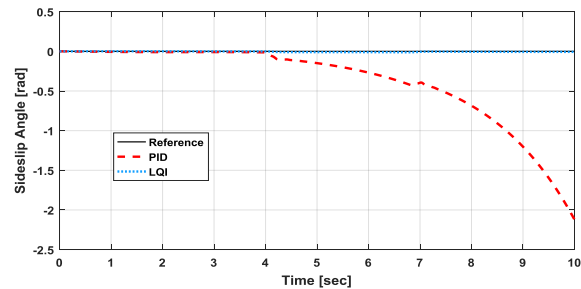


Figure 7. Sideslip angle performance on a wet road.

Figs. 6 and 7 show the results of the sideslip angle on dry and wet roads for both controllers. A comparison of RMSE for both simulations is shown in Table III. The acceptable limit for the sideslip angle is 10° or 0.175 rad; if it exceeds the limit, the tires will skid and make the vehicle lose controllability if it is not recovered as fast as possible. In Fig. 6, the PID controller tries to restrain the vehicle sideslip angle value at zero; however, when it reaches the external disturbance period, the vehicle loses stability and cannot recover after that period. Obviously, the vehicle system is worse under the wet road conditions, as shown in Fig. 7.

TABLE III. COMPARISON PERFORMANCE RMSE FOR SIDESLIP ANGLE

Sideslip angle	PID	LQI
Dry road (1.0μ)	2.421788	0.155124
Wet road (0.5μ)	11.91163	0.256117

As for the LQI controller, the vehicle system is still capable of restraining the sideslip angle, even at a low coefficient of friction, as shown in Fig. 7. The increment of RMSE percentage for the LQI controller between the dry road and the wet road is 60.5%, as shown in Table III, but it is still considered as controllable. In others word, the LQI controller is robust against crosswind external.

V. CONCLUSION

In this paper, a linear control design for SUVs was proposed and a validation method for DBC using MATLAB/Simulink simulation was presented. The PID and LQI controllers were tested in slalom test manoeuvres, and both controllers were found to be capable of overcoming the manoeuvre. However, the friction coefficient of the road affects the stability and handling of the SUV. Crosswind disturbances make the vehicle system become much worse, and this makes the controller reach the maximum capacity. As a result, the PID controller cannot overcome the lower friction coefficient with external disturbance injected into the system and loses its controllability. However, the LQI controller is still capable of enduring the test until the end with a lower RMSE and is robust against external disturbances.

ACKNOWLEDGEMENT

This work was supported by the Universiti Teknikal Malaysia Melaka (UTeM), Centre for Robotics and Industrial Automation and Ministry of Education are greatly acknowledged. The research was funded by Research Acculturation Grant Scheme Grant No. (RAGS/1/2015/TK0/UTEM/03/B00122).

REFERENCES

- [1] M. Z. Azmi et al., "Steering intervention strategy for side lane collision Avoidance," *ARNP J. Eng. Appl. Sci.*, vol. 12, no. 14, pp. 4265–4269, 2017.
- [2] J. Ryan, D. Bevely, and J. Lu, "Robust sideslip estimation using GPS road grade sensing to replace a pitch rate sensor," *Conf. Proc. - IEEE Int. Conf. Syst. Man Cybern.*, no. October, pp. 2026–2031, 2009.
- [3] D. Piyabongkarn, R. Rajamani, J. A. Grogg, and J. Y. Lew, "Development and experimental evaluation of a slip angle estimator for vehicle stability control," *IEEE Trans. Control Syst. Technol.*, vol. 17, no. 1, pp. 78–88, 2009.
- [4] Z. Sun and S.-K. Chen, "Automotive active safety systems: Introduction to the special section," *IEEE Control Syst. Mag.*, vol. 30, no. 4, pp. 36–37, 2010.
- [5] S. Zhu and Y. He, "Design of SUV differential braking controller considering the interactions of driver and control system," in *Proc. the ASME 2014 International Mechanical Engineering Congress and Exposition*, 2014, pp. 14–20.
- [6] B. Li, H. Du, and W. Li, "Fault-tolerant control of electric vehicles with in-wheel motors using actuator-grouping sliding mode controllers," *Mech. Syst. Signal Process.*, vol. 72–73, pp. 462–485, 2016.
- [7] S. Ding and J. Sun, "Direct yaw-moment control for 4WID electric vehicle via finite-time control technique," *Nonlinear Dyn.*, vol. 88, no. 1, pp. 239–254, 2017.
- [8] L. Li, X. Ran, K. Wu, J. Song, and Z. Han, "A novel fuzzy logic correctional algorithm for traction control systems on uneven low-friction road conditions," *Veh. Syst. Dyn.*, vol. 53, no. 6, pp. 711–733, 2015.
- [9] A. Aksjonov, K. Augsburg, and V. Vodovozov, "Design and simulation of the robust ABS and ESP fuzzy logic controller on the complex braking maneuvers," *Appl. Sci.*, vol. 6, no. 12, pp. 382, 2016.
- [10] L. Zhai, T. Sun, and J. Wang, "Electronic stability control based on motor driving and braking torque distribution for a four in-wheel motor drive electric vehicle," *IEEE Trans. Veh. Technol.*, vol. 65, no. 6, pp. 4726–4739, 2016.
- [11] W. Cao, Z. Liu, Y. Chang, and A. Szumanowski, "Direct yaw-moment control of all-wheel-independent-drive electric vehicles with network-induced delays through parameter-dependent fuzzy SMC design," *Math. Probl. Eng.*, vol. 2017, 2017.
- [12] A. Bagis, "Determination of the PID controller parameters by modified genetic algorithm for improved performance," *J. Inf. Sci. Eng.*, vol. 23, no. 5, pp. 1469–1480, 2007.
- [13] K. Arzén, "A simple event-based PID controller," in *Proc. 14th IFAC World Congr.*, vol. 18, pp. 423–428, 1999.
- [14] H. Kanchwala, J. Wideberg, C. B. Alba, and D. Marcos, "Control of an independent 4WD electric vehicle by DYC method," *Int. J. Veh. Syst. Model. Test.*, vol. 10, no. 2, pp. 168–184, 2015.
- [15] B. Zhu, L. T. Guo, J. Zhao, F. Gao, Z. Pan, and L. Q. Ren, "Direct yaw-moment control through optimal control allocation method for light vehicle," *Appl. Mech. Mater.*, vol. 246–247, pp. 847–852, 2012.
- [16] J. Chen, J. Song, L. Li, X. Ran, G. Jia, and K. Wu, "A novel pre-control method of vehicle dynamics stability based on critical stable velocity during transient steering maneuvering," *Chinese J. Mech. Eng.*, vol. 29, no. 3, pp. 475–485, 2016.
- [17] B. DO Anderson and J. B. Moore, *Optimal Control: Linear quadratic methods*, Courier Corporation, 2007.
- [18] L. Li, G. Jia, J. Chen, H. Zhu, D. Cao, and J. Song, "A novel vehicle dynamics stability control algorithm based on the hierarchical strategy with constrain of nonlinear tyre forces," *Veh. Syst. Dyn.*, vol. 3114, no. July, pp. 1–24, 2015.
- [19] N. Tavan, M. Tavan, and R. Hosseini, "An optimal integrated longitudinal and lateral dynamic controller development for vehicle path tracking," *Lat. Am. J. Solids Struct.*, vol. 12, no. 6, pp. 1006–1023, 2014.
- [20] Y. Hirano, "Development of an integrated control of front steering and torque vectoring differential gear system using modelica," pp. 17–26, 2017.
- [21] H. G. Malkapure and M. Chidambaram, "Comparison of two methods of incorporating an integral action in linear quadratic regulator," in *IFAC Proceedings Volumes*, 2014, vol. 47, pp. 55–61.
- [22] X. Ding and Y. He, "Application of driver-in-the-loop real-time simulations to the design of SUV differential braking controllers," *Intell. Robot. Appl.*, vol. 7506 LNAI, pp. 121–131, 2012.
- [23] C. Lin and C. L. Peng, "Stability control for Dual-Motor Independent Drive Electric Vehicle based on Sliding Mode Control," *Adv. Mater. Res.*, vol. 655–657, pp. 1403–1409, 2013.
- [24] N. M. B. A. Ghani, N. M. Ghani, Y. Sam, and A. Ahmad, "Active steering for vehicle system using Sliding Mode Control," no. May, pp. 27–28, 2006.
- [25] M. Shino, N. Miyamoto, Y. Q. Wang, and M. Nagai, "Traction control of electric vehicles considering vehicle stability," 6th Int. Work. Adv. Motion Control Proc., pp. 311–316, 2000.



Mohd Firdaus Omar received his B.Eng. degree in mechanical engineering technology (automotive) from Universiti Teknikal Malaysia Melaka (UTeM) in 2015. Currently, he is pursuing his master's degree in electrical engineering at the same university.